Retromodified Residues: Small Peptides and Polymers. Interactions, Force-Field Parametrization and Conformational Analyses

Carlos Alemán* and Jordi Puiggalí*

Departament de Enginyería Química, E.T.S.I.I.B., Universitat Politècnica de Catalunya, Avgda Diagonal 647, Barcelona 08028, Spain

Received July 22, 1994 (Revised Manuscript Received November 16, 1994®)

Suitable parameters for describing the conformational behavior of bis(acetamide) and malonamide retro-amide residues are obtained and tested. For this purpose, bonded parameters, *i.e.* stretching, bending, and torsion, were computed with the PAPQMD (program for approximate parametrization from quantum mechanical data) strategy and compared with experimentally derived force-field parameters for residues without retro-amide link. Electrostatic parameters were determined by fitting the Coulombic monopole–monopole electrostatic potential to the quantum mechanical electrostatic potential computed from both ab initio 6-31G* and semiempirical MNDO wave functions. In addition, the variation of the atomic charges with the conformation was investigated. Equilibrium geometries and thermodynamic properties for bis(acetamido)methane and *N,N'*-dimethylmalonamide obtained from molecular mechanical calculations using the derived parameters were compared with available experimental and quantum mechanical data. The selected parameters were then applied to the study of (i) the retro-dipeptides bis(acetamido)ethane and bis(acetamido)propane and (ii) the crystalline structure of several aliphatic polyamides. The conformational trends obtained for bis(acetamido)ethane and bis(acetamido)propane using ab initio and semiempirical quantum mechanical methods are in good agreement with the molecular mechanical results. Moreover, the minimal energy structures for nylon 1,3 and 1,5 on a solid-state model allowed us to explain the X-ray-refined data using the least-atom-linked-squares methods.

Introduction

Retro-amide links have successfully been incorporated in the synthesis of bioactive peptide analogs[1] such as LHRH,[2] enkephalinamides,[3] substance P,[4] somatostatin,[5] gastrin,[6] or peptide sweeteners.[7] Within this framework, both bis(acetamide) and malonamide residues, as well as their derivatives, are of considerable interest in the synthesis of peptidomimetic compounds.[2-4,8,9] They can be considered as the glycine residue (see Figure 1) to which one of the peptide groups that link it to neighboring residues has been inverted (retromodification). However, these symmetric retro residues exhibit a variety of conformational patterns.

The structure of some small bis(acetamide)[10] and malonamide[9,11,12-15] derivatives has been determined by X-ray crystallography. Thus, the bis(acetamido)methane (BAAM) molecule assumes two nearly identical, symmetric conformations with planar trans amide groups and $\varphi_1 = \varphi_2$. On the other hand, small malonamide derivatives are ususally asymmetric with two different torsional angles ψ_1 and ψ_2, which nevertheless have similar values in different compounds. Thus, each of the two peptide bonds is involved in an infinite network of hydrogen

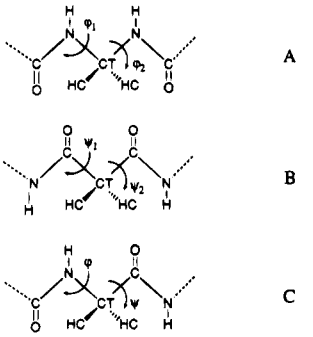

Figure 1. Schematic structures of the bis(acetamide) (A), malonamide (B), and glycine (C) residues. The corresponding atom types are also indicated.

® Abstract published in *Advance ACS Abstracts,* January 1, 1995.

(1) Goodman, M.; Chorev, M. *Acc. Chem. Res.* **1979**, *12*, 1.
(2) Chaturvedi, N.; Goodman, M.; Browers, C. *Int. J. Peptide Protein Res.* **1981**, *17*, 72.
(3) Chorev, M.; Shavitz, R.; Goodman, M.; Minick, S.; Guillemin, R. *Science,* **1979**, *204*, 1210.
(4) (a) Chorev, M.; Rubini, E.; Gilon, C.; Wormser, U.; Selinger, Z. *J. Med. Chem.* **1983**, *26*, 129. (b) Chorev, M.; Yacon, M.; Wormser, U.; Levian-Teitelbaun, D.; Gilon, C.; Selinger, Z. *Eur. J. Med. Chem.* **1986**, *21*, 96.
(5) (a) Pallai, P.; Structhers, S.; Goodman, M.; Vale, W. *Biopolymers* **1983**, *22*, 2523. (b) Pallai, P.; Struthers, S.; Goodman, M.; Moroderi, M.; Wunsch, E.; Vale, W. *Biochemistry* **1985**, *24*, 1933.
(6) Rodriguez, M.; Dubreil, P.; Bali, J.-P.; Martinez, J. *J. Med. Chem.* **1987**, *30*, 758.
(7) (a) Benedetti, E.; Di Blasio, B.; Pavone, V.; Pedone, C.; Fuller, W. D.; Mierke, D. F.; Goodman, M. *J. Am. Chem. Soc.* **1987**, *109*, 4712. (b) Goodman, M.; Coddington, J.; Mierke, D. F.; Fuller, W. D. *J. Am. Chem. Soc.* **1987**, *109*, 4712.
(8) (a) Berman, J.; Goodman, M. *Int. J. Peptide Protein Res.* **1984**, *23*, 610.
(9) Gomez, E. J.; Vitoux, B.; Marraud, M.; Sarakellos, C.; El-Masdouri, L.; Aubry, A. *Int. J. Peptide Protein Res.* **1989**, *34*, 480.
(10) El-Masdouri, L.; Aubry, A.; Gomez, E.; Vitoux, B.; Marraud, M. *Acta Crystallogr.* **1992**, *C48*, 176.
(11) (a) Ruigin, W.; Chang, H.; Shengua, S.; Kailiang, S.; Lei, S. *J. Chem. Struct.* **1988**, *7*, 36. (b) Chich, P. C.; Subramanian, E.; Trotter, J. J. *Chem. Soc.* **1970**, 179. (c) El-Masdouri, L.; Aubry, A.; Gomez, E. J.; Vitoux, B.; Marraud, M. *J. Chim. Phys.* **1988**, *85*, 583.
(12) Dado, G. P.; Desper, J. M.; Holmgren, S. K.; Rito, C. J.; Gellman, S. H. *J. Am. Chem. Soc.* **1992**, *114*, 4834 and references therein.
(13) (a) Kalman, A.; Argay, G.; Fischer, E. *Acta Crystallogr. Sect. C* **1985**, *41*, 1648. (b) Gieven, V. A.; Daveder, B. *Acta Crystallogr. Sect. B* **1978**, *34*, 533.
(14) Alemán, C.; Perez, J. J. *J. Mol. Struct.* **1994**, *304*, 17.
(15) Tereshko, V.; Navarro, E.; Puiggalí, J.; Subirana, J. A. *Macromolecules* **1993**, *26*, 7024.

0022-3263/95/1960-0910$09.00/0

bonds. In addition, the potential energy surfaces of the BAAM[15] and *N,N'*-dimethylmalonamide (DMMA),[16,17] as well as the α-alkyl and α,α-dialkyl derivatives of the latter,[18] have been studied using quantum mechanical (QM) methods at the semiempirical and ab initio levels. The results showed similar trends to those observed by X-ray analysis. However, in this case they are the result of the formation of an intramolecular six-membered hydrogen-bonded system, which disturbs the internal symmetry of the molecule. Thus, BAAM behaves symmetrically with $\varphi_1 = \varphi_2$, whereas all the malonamide derivatives tend to adopt a strongly asymmetric conformation with $\psi_1 \neq \psi_2$. On the other hand, comparison of the structures obtained from X-ray diffraction and QM data with those derived using force-field (FF) methods[19,20] reveals serious discrepancies. These were attributed to some deficiencies in the FF parameters,[14,16,17] which give a poor description of the excessive attractive interactions, *i.e.* C=O···H−N, or the excessive repulsive interactions, *i.e.* C=O···O=C and N−H···H−N. Consequently, a rigorous and explicit FF parametrization is required for a better description of the conformational properties of these small peptides using FF methods. Furthermore, little is known about the conformational preferences of some small retro-peptides like those derived from α- and α,α-alkylation of BAAM: bis(acetamido)ethane (BAAE) and bis(acetamido)propane (BAAP).

On the other hand, residues with retro-amide links are also the basic units of some aliphatic polyamides (nylons) which are closely related with fibrous proteins. In the last few years we have studied nylons with unconventional structures, *e.g.* layered α, β, or γ structures.[21,22] Different conformations have been found in polyamides which contain a single methylene unit between two amide groups. Their strong interactions may influence the conformational properties of these polymers. Thus, alternating copolyamides containing glycine (nylons 2/3, 2/6, 2/11, and 2/12) assume a polyglycine II structure characterized by a three-dimensional network of hydrogen bonds, which tightens the whole structure.[23] Polyamides derived from malonic residues (nylons *n*,3) appear to be polymorphic, even though a characteristic conformation with a double hydrogen-bond direction is preferred.[15,24] The copolymers of diaminomethane and α,ω-dicarboxylic acids (nylons 1,*n*) are another family of polyamides which also have a methylene group between amide units:

$$\text{-CONHCH}_2\text{NHCO(CH}_2)_{n-2}\text{-}$$

Several members of this family of polymers have been studied and characterizated by X-ray and electron diffraction.[25-30] Approximate models of these polymers were refined using the least-atom-linked-squares (LALS) methods.[31] The results suggest that the single methylene group always takes the characteristic conformation of the BAAM, whereas the conformation of the dicarboxylic unit is variable. So, structures with one or three hydrogen-bond directions appear to be stabilized when the number of methylene groups is even or odd, respectively.[30] Nevertheless, since the conformational refinement in the LALS method is rather crude and the number of diffraction spots is low, another criterion is required in order to descriminate between the different models compatible with the experimental data. In this sense, energy calculations using FF-derived techniques, *e.g.* molecular mechanics (MM) and molecular dynamics (MD), have been a poweful tools in the analysis of the crystal structures of several related polyamides.[32] In addition, these methods could provide a more complete description of the molecular conformation at microscopic level, since poor crystallographic data are usually obtained from polymer fibers.

FF-derived techniques are based on the implicit assumption that the energy of a system can be represented as the addition of two contributions: (i) the bonded term, which includes the energy of stretching, bending, and proper and improper torsion, and (ii) the nonbonded term, where the electrostatic, hydrogen-bond, and van der Waals energies are considered. The equations used to define the different contributions (the force-field) are of extreme simplicity, which explains the speed of FF-based calculations, and so it is possible to analyze large and complex structures. All the analytical expressions used to compute both the bonded and nonbonded terms include several parameters. Therefore, the study of any molecular system by MM or MD techniques requires the previous knowledge of all the parameters decribing such a system. This leads to one of the most serious shortcomings of FF-derived techniques, since although large parameter data sets are available for biological molecules, *e.g.* proteins and DNA, parameters describing less common residues are often not available or have been approximated using simple nonstandard procedures, which would preclude their study by FF-derived methods.

A rigorous FF parametrization should be based on experimental data, since the ultimate goal of the FF-derived methods is to reproduce, explain, and predict experimental evidence. However, in most cases this is not possible due to the lack of experimental data. Quantum mechanical (QM) based parametrization ap-

(16) Alemán, C.; Pérez, J. J. *Int. J. Peptide Protein Res.* **1993**, *41*, 606.
(17) Alemán, C.; Pérez, J. J. *J. Mol. Struct.* **1993**, *285*, 221.
(18) Alemán, C.; Perez, J. J. *Int. J. Peptide Protein Res.* **1994**, *43*, 258.
(19) Stern, P. S.; Chorev, M.; Goodman, M.; Hagler, A. T. *Biopolymers* **1983**, *22*, 1885.
(20) Osguthorpe, P. D.; Campbell, M. M.; Osguthorpe, D. J. *Int. J. Peptide Protein Res.* **1991**, *38*, 357.
(21) Bunn, C. W.; Garner, E. V. *Proc. R. Soc. London* **1947**, *A189*, 39.
(22) Kinoshita, Y. *Makromol. Chem.* **1959**, *33*, 1.
(23) (a) Puiggalí, J.; Muñoz-Guerra, S.; Lotz, B. *Macromolecules* **1986**, *19*, 119. (b) Puiggalí, J.; Muñoz-Guerra, S.; Subirana, J. A. *Polymer* **1987**, *28*, 209. (c) Muñoz-Guerra, S.; Fita, I.; Aymami, J.; Puiggalí, J. *Macromolecules* **1988**, *21*, 1563. (d) Bermudez, M.; Puiggalí, J.; Muñoz-Guerra, S. Submitted work. (e) Puiggalí, J.; Muñoz-Guerra, S. *J. Polym. Sci., Part B: Polym. Phys.* **1989**, *27*, 1563. (f) Bella, J.; Puiggalí, J.; Subirana, J. A. *Polymer* **1994**, *35*, 1291.
(24) Puiggalí, J.; Aceituno, J. E.; Franco, L.; Lloveras, J.; Prieto, A.; Vidal, X.; Xenopoulus, A.; Fernández-Santín, J. M.; Subirana, J. A. *Progr. Collect. Polym. Sci.* **1992**, *87*, 35.
(25) Puiggalí, J.; Muñoz-Guerra, S. *J. Polym. Sci., Part B: Polym. Phys.* **1987**, *25*, 513.
(26) Puiggalí, J.; Muñoz-Guerra, S.; Subirana, J. A. *J. Polym. Sci., Part A: Polym. Chem.* **1987**, *25*, 1445.
(27) Franco, L.; Aceituno, J. E.; Subirana, J. A.; Puiggalí, J. *Polymer Preprints* **1992**, *31*, 325.
(28) Franco, L.; Navarro, E.; Subirana, J. A.; Puiggalí, J. *Macromolecules* **1994**, *27*, 4284.
(29) Alemán, C.; Bella, J. *Biopolymers* **1994**, in press.
(30) Alemán, C.; Franco, L.; Puiggalí, J. *Macromolecules* **1994**, *27*, 4298.
(31) Campbell-Smith, P.; Arnott, S. *Acta Crystallogr. Sect. A* **1978**, *34*, 3.
(32) (a) Bella, J.; Alemán, C.; Alegre, C.; Fernández-Santín, J. M.; Subirana, J. A. *Macromolecules* **1992**, 25, 5225. (b) Alemán, C.; Bella, J.; Perez, J. J. *Polymer* **1994**, *35*, 2596. (c) López-Carrasquero, F.; Martinez-Ilarduya, A.; Alemán, C.; Muñoz-Guerra, S. *Macromol. Chem. Phys.* 1995, in press.

pears to be a suitable alternative, since (i) QM data are always accessible; (ii) the parametrization can be performed on any system; (iii) the effect of the molecular and extramolecular environment can be taken into account;[33-35] and (iv) when some experimental data are available, such information can be incorporated in the parametrization[36,37] to correct some QM-derived results. The shortcomings of the QM-based parametrization are those inherent to approximations of QM methods (for a recent review, see ref 36).

In spite of the chemical and structural interest of retro-amide compounds, no FF allowing a rigorous conformational analysis of retro-peptides and related polyamides *e.g.* nylons 1,*n* and *n*,3, has been available until now. Here we report the bonded and nonbonded parameters required for MM and MD calculations of retro-amide compounds. The experimetal parametrization of these molecules is still impossible due to the scarcity of experimental data. Therefore, all the parameters were obtained using QM calculations. These parameters were tested on two model compounds: BAAM and DMMA. Subsequently, they were used in the study of (i) the conformational and energetic properties of the retro-dipeptides BAAE and BAAP and (ii) the crystalline structure of several aliphatic polyamides *i.e.* nylons 1,3 and 1,5, in order to verify and improve the models obtained using LALS refinements.

Computations

Ab initio wave functions were computed with the HONDO 7.0[38] molecular orbital package. AM1 calculations were carried out using a locally modified version of the MOPAC computer program.[39,40] The determination of bonded FF parameters was performed using the PAPQMD program.[33] Molecular electrostatic potentials (MEPs) and atomic point charges were determined using the MOPETE and MOTODO programs.[41] MM calculations were performed with the AMBER 3.0A set of programs.[42] Entropies and heat capacities were computed using the NMODE module of the AMBER 3.0A computer programs and the THERMO module of the MOPAC computer programs. In all cases a temperature of 298 K was considered.

Approximate models for nylon 1,3 and 1,5 with a sound stereochemistry were build and then refined using the LALS method.[31] Standard bond lengths and angles for polyamides were adopted to build the repeating unit and were held fixed throughout the modeling process. The models were refined according to the experimental chain repeat length (6.0 and 8.7 Å), the packing constraints due to the unit cell dimensions, and the optimum hydrogen-bond geometry. Electron diffraction data were also used to test and improve the quality of the models.

All the calculations were perfomed in the IBM 3090/600VF at the Centre de Supercomputació de Catalunya (CESCA) and in the HP/300 in our laboratory.

Interactions and Force-Field Parametrization

In a preliminary approach, FF parameters for the bis(acetamide) and malonamide residues should be taken from those of glycine by a homology strategy.[43] Nevertheless, both the strong inductive effects generated by the retromodification[44] and the restricted conformational spaces accessible to the residues[14,17] suggest that some parameters defining pure interactions, such as torsional barriers and atomic charges, could change with respect to those of glycine, making necessary an explicit and complete parametrization.

Analytical Expression and Atom Types of the Force Field. Classical energies were computed using the following analytical potential function (see ref 45) of the AMBER FF:[46,47]

$$E_{TOT} = \sum_{bonds} K_r(r_{ij} - r_{ij}^{eq})^2 + \sum_{angles} K_\theta(\theta_{ijk} - \theta_{ijk}^{eq})^2 + \sum_{dihedrals} \frac{V_n}{2}[1 + \cos(n\phi - \gamma)] \sum_{nonbonded}\left[\frac{A_{ij}}{R_{ij}^{12}} - \frac{B_{ij}}{R_{ij}^{6}} + \frac{qiqj}{\epsilon R_{ij}}\right] + \sum_{H\text{-}bonds}\left[\frac{C_{ij}}{R_{ij}^{12}} - \frac{D_{ij}}{R_{ij}^{10}}\right] \quad (1)$$

where the first two sums represent the harmonic approximation for stretching and bending terms, followed by a Fourier series expansion for the torsional term, which allows different *n* values to be considered if needed. The second part of the expression contains the Lennard-Jones and the electrostatic terms as well as a 10-12 H-bond term. This potential function has been used in MM and MD studies of polyamides.[32,48]

A minimal choice was performed in order to start developing the FF. In this respect, the atom types needed are displayed in Figure 1. Of course, this hypothesis was to be tested and retained or rejected, depending on the results obtained. Atom types for a glycine unit are also shown for comparison.

Stretching and Bending Terms. The equilibrium bonds and angles and the stretching and bending force parameters required for retro-peptides and derived polyamides are displayed in Table 1. Small changes in stretching and bending parameters should be anticipated for bis(acetamide) and malonamide residues when compared with glycine, owing to the low effect of the retromodification in the bond strength between two atom types. Therefore, stretching and bending parameters

(33) Alemán, C.; Canela, E. I.; Franco, R.; Orozco, M. *J. Comput. Chem.* **1991**, *12*, 664.
(34) Alemán, C.; Orozco, M. *J. Comput. Aided Mol. Design* **1992**, *6*, 331.
(35) Alemán, C.; Orozco, M. *Biopolymers* **1994**, in press.
(36) Orozco, M.; Alemán, C.; Luque, F. J. *Models Chem.* **1993**, *130*, 695.
(37) Dillen, J. L. M. *J. Comput. Chem.* **1992**, *13*, 257.
(38) Dupuis, M.; Watts, J. D.; Villar, H. O.; Hurst, G. J. B. HONDO 7.0, 1987.
(39) Olivella, S. *QCPE Bull.* **1984**, *4*, 109. Extended by Olivella, S. and Bofill, J. M., 1990.
(40) Stewart, J. J. P. *QCPE Bull.* **1983**, *3*, 101.
(41) Luque, F. J.; Orozco, M. Unpublished results.
(42) Kollman, P. AMBER 3.0A Computer Program, University of California, San Francisco, 1990.
(43) O'Donnell, T. J.; Rao, S. N.; Koecher, K.; Martin, Y. C.; Eccler, B. *J. Comput. Chem.* **1991**, *12*, 209.
(44) Stern, P. S.; Chorev, M.; Goodman, M.; Hagler, A. T. *Biopolymers* **1983**, *22*, 1901.
(45) K_r is the stretching constant for the $i-j$ bond, r_{ij} is the length of the $i-j$ bond, r_{ij}^{eq} is the length for the bond type $i-j$ corresponding to the minimum energy. K_θ is the bending constant for the $i-j-k$ angle, θ_{ijk} is the value of the $i-j-k$ bond angle, θ_{ijk}^{eq} is the value of the $i-j-k$ angle corresponding to the minimum energy. V_n is the torsional energy barrier of the n-Fourier term for the rotation around the bond, γ is the angle phase of the n-Fourier term, which determines the torsion angle of maximum energy, ϕ is the torsion angle. A_{ij} and B_{ij} are the van der Waals parameters, q_i and q_j are fractional charges localized at the nuclei, C_{ij} and D_{ij} are the hydrogen-bond parameters, R_{ij} is the distance between atoms i and j.
(46) Weiner, S. J.; Kollman, P. A.; Nguyen, D. T.; Case, P. A. *J. Comput. Chem.* **1987**, *8*, 581.
(47) Weiner, S. J.; Kollman, P. T.; Case, P. A.; Singh, U. C.; Ghio, C.; Alagona, G. *J. Am. Chem. Soc.* **1984**, *106*, 765.
(48) (a) Alemán, C.; Subirana, J. A.; Perez, J. J. *Biopolymers* **1992**, *32*, 621. (b) Alemán, C.; Perez, J. J. *Biopolymers* **1993**, *33*, 1811.
(49) Binkley, J. S.; Pople, J. A.; Hehre, W. J. *J. Am. Chem. Soc.* **1980**, *102*, 939.

Table 1. Equilibrium Bond Lengths and Angles and Stretching and Bending Force Parameters for Bis(acetamide) and Malonamide Residues (see Figure 1)[a]

stretching/bending	Eq(QM)	Eq(A)	K(QM)	K(A)
C–N	1.349	1.335	507	490
C=O	1.215	1.229	867	570
N–H	0.996	1.010	527	434
N–CT	1.468	1.449	308	337
CT–HC	1.084	1.090	362	331
C–CT	1.516	1.522	310	317
CT–CT[b]	1.528	1.526	300	310
C–N–CT	120.1	121.9	72	80
O=C–N	124.1	122.9	99	80
C–N–H	119.3	119.8	46	35
H–N–CT	119.3	118.4	45	38
N–CT–N	109.1		40	
N–CT–HC	109.5	109.5	42	35
HC–CT–HC	109.5	109.5	49	35
N–C–CT	113.9	116.9	70	70
O–C–CT	123.9	120.4	69	30
C–CT–HC	109.5	109.5	51	35
C–CT–CT[b]	110.0	111.1	69	63
HC–CT–CT[b]	109.5	109.5	53	35
CT–CT–CT[b]	109.5	109.5	77	40
C–CT–C	111.9		100	

[a] QM means quantum mechanical and A means AMBER force field. Distances are in angstroms, angles in degrees, stretching force parameters in kcal/mol·Å^2, and bending force parameters in kcal/mol·rad^2. [b] Stretching and bending parameters for the aliphatic groups of nylons 1,*n* and *n*,3.

provided in the AMBER-FF for glycine were transferred to the compounds under study. However, additional parameters were required, *i.e.* N–CT–N and C–CT–C. These were derived from QM calculations. Thus, in order to make a reliable comparison between QM and AMBER parameters, complete parametrizations of bis(acetamide) and malonamide were performed. This permits (i) confirmation of the general similarity and good correlation of the stretching and bending FF parameters obtained from QM data with the values reported in AMBER-FF for glycine and (ii) reliable values for the missing parameters.

r_{eq} and θ_{eq} were obtained from SCF-MO (self consistent field molecular orbital) geometry optimizations of small model molecules using the 3-21G[47] basis set. Results are displayed in Table 1. There is clear agreement between QM and empirical equilibrium parameters. Thus, considering the precision of the FF calculations, all the differences found can be considered negligible.

Table 1 also reports stretching and bending force parameters which have been derived from ab initio SCF-MO data using the standard PAPQMD (program for approximate parametrization from quantum mechanical data) strategy.[33,34] Accordingly, each bond and angle type was perturbed from its equilibrium geometry. The energy of these perturbated structures was then computed at the RHF (restricted Hartree–Fock) level with the 3-21G basis set, which yields the QM perturbational energy for each geometry: ΔE^{QM} (see eq 2). The whole of ΔE^{QM} is then fitted to the FF (in this case an AMBER-type FF, see eq 1), in which all the parameters are changed until the difference between FF and QM energies is minimal. For each bond and angle, six perturbed geometries were considered. The large perturbations were 0.20 Å (single bonds), 0.15 Å (double bonds), and 15° (angles).

$$(\Delta E^{QM} - \Delta E^{FF})^2 = \text{minimum} \qquad (2)$$

There is marked agreement between empirical stretching force parameters and the PAPQMD/3-21G parameters, even thougth the latter are usually larger than AMBER values, as expected from the neglection of correlation effects in SCF-MO calculations.[34,50,51] The worst agreement is found for the C=O bond, whose strength seems to be largely overestimated in PAPQMD/3-21G calculations. The obvious failure of the PAPQMD/3-21G method to represent the stretching bonds like the C=O is due to the poor ability of the RHF wave function to represent the stretching of double bonds.[50]

Comparison between the bending parameters obtained from PAPQMD/3-21G calculations and the experimentally derived values reported in AMBER suggest that the first would probably need to be scaled. Thus, the results indicate an overestimation of the strength of bending force constants arising from the use of SCF wave functions. However, no clear correlation was found between PAPQMD/3-21G and AMBER bending parameters. Similar findings were recently reported in FF parametrization studies.[34,35] Thus, in these works the authors found a very poor intercorrelation between different empirically derived FFs, *i.e.* AMBER,[46,47] CHARM,[52] TRIPOS,[53] and MM2.[54] This clearly indicates that most of the fine parametrization process in empirical FFs was performed in the stretching term and that a finer parametrization of the bending term was considered unnecessary. Consequently, we directly apply the PAPQMD/3-21G bending force constants for the missing parameters N–CT–N and C–CT–C.

In summary, these results demonstrated the general similarity of the stretching and bending FF parameters obtained for bis(acetamide) and malonamide residues with those reported empirically for glycine. Furthermore, the PAPQMD/3-21G is a suitable strategy for evaluating the missing bonding FF parameters needed to perform MM or MD studies on large molecules such as polypeptides and organic polymers, in cases where the scarce amount of experimental data makes empirical parametrization impossible.

Torsional Term. Recently, a great deal of computational effort has been devoted to the QM parametrization of torsions in FF developed for proteins,[55,56] where the trans–cis isomerism of the peptide bond[56] appears to be an essential factor in protein folding.[57] The rotation of the peptide bond in retro-peptides has been considered to be analogous to that in proteins and has been assumed to be equal to that reported in AMBER FF. On the other hand, the rotation around the φ_i and ψ_i angles in bis(acetamide) and malonamide is crucial, since they could be altered by the inductive effects of the retro-amide link. In order to investigate these alterations, we computed the potential energy barriers for the rotation around the

(50) Orozco, M.; Luqu, F. J. *J. Comput. Chem.* **1993**, *14*, 881.
(51) Casanovas, J.; Alemán, C. Submitted work.
(52) (a) Brooks, B. R.; Bruccoleri, R. E.; Olafson, B. D.; States, D. J.; Swaminathan, S.; Karplus, M. *J. Comput. Chem.* **1983**, *4*, 187. (b) Nilsson, L.; Karplus, M. *J. Comput. Chem.* **1986**, *7*, 591.
(53) Clark, M.; Cramer, R. D., III; Opdenbusch, N. *J. Comput. Chem.* **1989**, *10*, 982.
(54) (a) Allinger, N. L. *J. Am. Chem. Soc.* **1977**, *99*, 8127. (b) Sprague, J. T.; Tai, J. C.; Yuth, Y. H.; Allinger, N. L. *J. Comput. Chem.* **1977**, *8*, 581.
(55) (a) Schäfer, L.; Alsen, C. V.; Scarsdale, J. N. *J. Chem. Phys.* **1982**, *76*, 1439. (b) Hensen, J. H.; Gordon, M. S. *J. Am. Chem. Soc.* **1991**, *113*, 7917.
(56) (a) Luque, F. J.; Orozco, M. *J. Org. Chem.* **1993**, *58*, 6397. (b) Wiberg, K. B.; Brenemon, C. M. *J. Am. Chem. Soc.* **1992**, *114*, 831. (c) Dufi, E. M.; Severance, D. L.; Jorgensen, W. L. *J. Am. Chem. Soc.* **1992**, *114*, 7535.
(57) (a) Bachinger, H. P. *J. Biol. Chem.* **1987**, *262*, 17144. (b) Lang, K.; Schmide, F. X.; Fischer, G. *Nature* **1987**, *329*, 268.

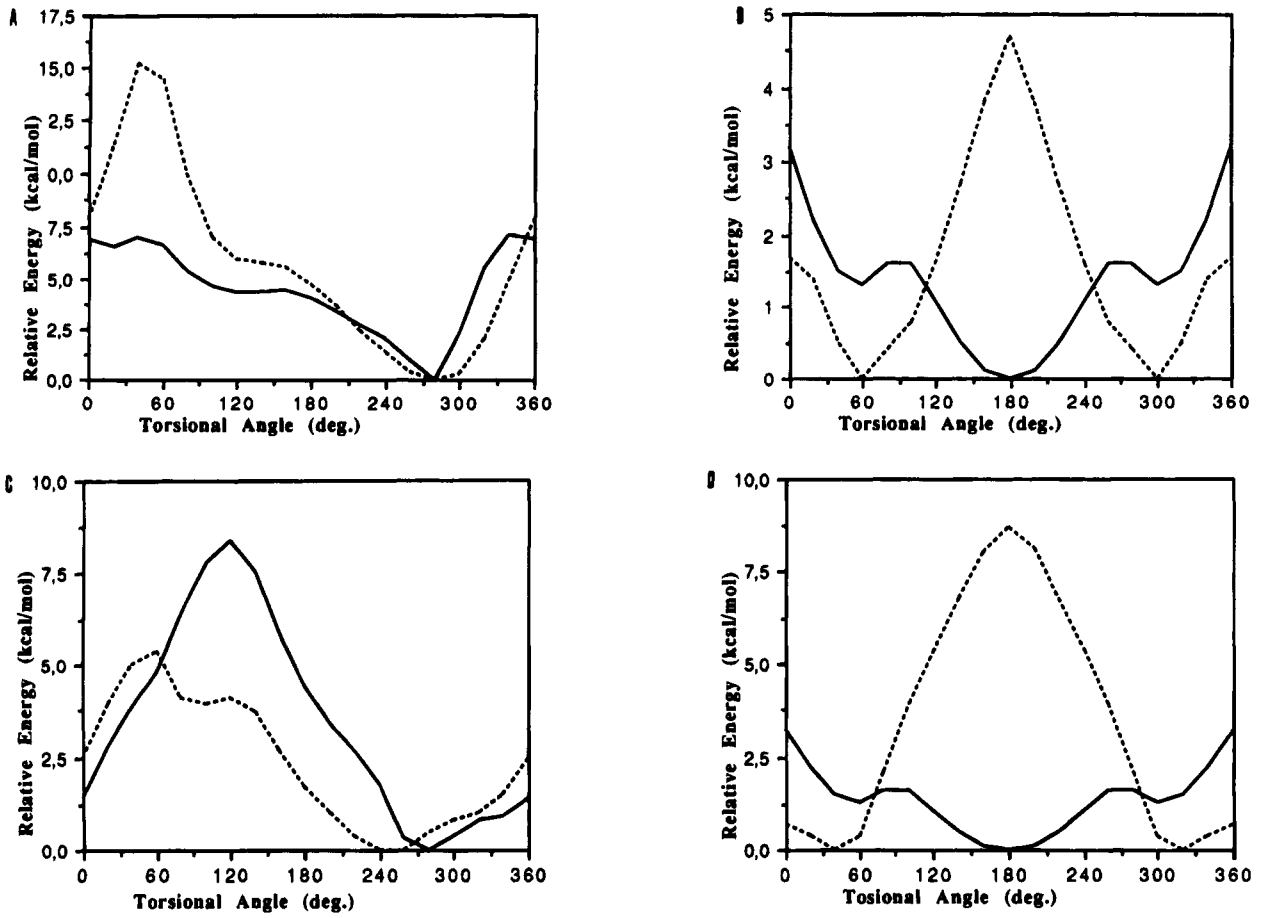

Figure 2. Potential energy profiles for bis(acetamido)methane (A, B) and *N,N'*-dimethylmalonamide (C, D) computed with the AM1 method. Comparison between retro-dipeptide (solid line) and glycine dipeptide (dashed line) is shown in each picture. The dihedral angles fixed were (A) $\varphi_2 = 60°$ (solid line) and $\psi = 60°$ (dashed line); (B) $\varphi_2 = 180°$ (solid line) and $\psi = 180°$ (dashed line); (C) $\psi_2 = 60°$ (solid line) and $\varphi = 60°$ (dashed line); (D) $\psi_2 = 180°$ (solid line) and $\varphi = 180°$ (dashed line).

bonds N−CT and C−CT in BAAM and DMMA (see Figure 1), respectively. The same calculations were performed in *N*-acetyl-*N'*-methylglycinamide for comparison.

The ability of the RHF-SCF methods to describe the whole rotation pathway around single bonds is well known.[58] More specifically, we used the AM1 semiempirical method[59] which provides good estimates of barriers for single bonds.[33,34,59,60] Several energy profiles were computed for the φ_1 and ψ_1 angles of each molecule, keeping φ_2 and ψ_2 fixed at different values. In particular, a total of 18 torsional profiles were computed for each model molecule, *i.e.* using a grid of 20° on the fixed dihedral angle. In all cases the results are similar to those displayed in Figure 2, where φ_2 and ψ_2 were kept at 60° (parts A and C) and 180° (parts B and D).

The energy profiles obtained for the rotation around the N−CT of bis(acetamide) and glycine dipeptides are shown in Figure 2, parts A and B. The first compound presents higher energy barriers. However, when $\varphi_2 = 60°$ (ψ for glycine), profiles with the same periodicity were obtained for both dipeptides. In contrast, when φ_2=180°, the energy profiles displayed different periodicity. Thus, at $\varphi = \psi = 180°$, glycine forms a five-membered intramolecular hydrogen bond, whereas this conformation is unfavorable for bis(acetamide) because there is a strong repulsion between the two hydrogens. On the other hand, the energy profiles computed for the rotation around the C−CT are displayed in Figure 2, parts C and D. The results are similar to those discussed for bis(acetamide). This may be attributed to the strong atomic contacts between the oxygen atoms in malonamide dipeptide.

The torsional parameters were computed from a four-term Fourier expansion[45] using the PAPQMD strategy.[33] The variation of all nonbonded terms was taken into account using the perturbational correction of the energy implemented in PAPQMD computer program. We used a general parameters strategy according to which all the dihedral angles $\{A_i\}$−B−C−$\{D_i\}$ have the same parameters, *i.e.* only the nature of the two central atoms is considered. The relevant $V_n/2$ parameters, the value of the phase (γ), and of the periodicity (n) are reported in Table 2. The application of the PAPQMD strategy leads to very similar results to the experimental data for glycine using AMBER FF. This seems indicate that the characteristics of the potential energy profiles obtained for retro-peptides must be attributed basically to the strong hydrogen−hydrogen and oxygen−oxygen nonbonded interactions, *i.e.* van der Waals and electrostatics, rather than the rotations of the N−CT and C−CT single bonds proper.

(58) Hehre, W. J.; Radom, L.; Scheleyer, P. v. R.; Pople, J. A. In *Ab initio Molecular Orbital Theory*; Wiley: New York, 1986, and references there in.
(59) Dewar, M. J. S.; Zoebisch, E. G.; Healy, E. E.; Stewart, J. J. P. *J. Am. Chem. Soc.* **1985**, *107*, 3902.
(60) Pranata, J.; Jorgensen, W. L. *J. Am. Chem. Soc.* **1991**, *113*, 9483.

Table 2. Torsional Parameters for Bis(acetamide) and Malonamide Units (see Figure 1)[a]

dihedral	method	$V_n/2$	γ	n
-N-CT-	PAPQMD/AM1	0.2	0	3
	AMBER FF[b]	0.0	0	3
-C-CT-	PAPQMD/AM1	0.4	0	2
	AMBER FF[b]	0.0	0	2

[a] $V_n/2$ in kcal/mol. [b] Taken from AMBER force field[46,47] (see text).

Electrostatic Term. The electrostatic is the most important interaction in most systems and consequently requires accurate parametrization. Inadequate atomic charges drastically reduce the quality of the results derived from any MM or MD analysis. It is difficult to assign charges based on experimental data because of the poor resolution of X-ray diffraction maps,[61] therefore they must be determined by theoretical methods. In the present work we use the strategy developed by Momany[62] according to which the atomic charges (electrostatic charges) are derived by fitting the rigorously defined QM molecular electrostatic potential (MEP) to the Coulombic monopole-monopole electrostatic potential. To perform this fitting, the MEP was evaluated at points located at four Connolly layers.[63] The inner layer was placed at 1.4 times the van der Waals radii of the atoms and a separation of 0.2 Å between layers was considered, a density of 2.0 points/Å^2 in each layer being defined. The ability of the electrostatic charges computed either from ab initio[64-66] or from semiempirical[67-70] wave functions to provide an accurate description of the electrostatic properties has been demonstrated.

The molecular wave function and the electrostatic properties vary with the conformation, and therefore atomic charges are also sensitive to the conformational changes. This has recently been studied for several amino acidic residues, *i.e.* glycine,[71] alanine,[72] and α-aminoisobutyric acid.[73] The modification of a glycine residue by its retro-analog with formation of bis(acetamide) or malonamide results in a substantial conformational change. On the other hand, the retromodification induces by itself a strong change in the atomic charge of the α-carbon. This was discussed from a qualitative point of view by Stern et al.,[74] using partial charges derived from a Mulliken population analysis. Thus, in the first step we analyze the changes on the atomic point charges induced by the retromodification and their variation with molecular conformation in both BAAM and DMMA model peptides. For this purpose various conformations were generated. These include (i) the unique minimum energy structure, which was characterized from ab initio calculations[14,17] (conformers **I**), and (ii) some typical conformations found in polypeptide structures, *i.e.* parallel pleated sheet (**II**), antiparallel pleated sheet (**III**), and α-helix (**IV**),[75] which were built using standard bond distances and angles. The ab initio 6-31G* [76] wave functions calculated at each geometry were used to compute the rigorous QM-MEP. Results are shown in Tables 3 and 4.

Table 3 shows the energies, dihedral angles, and electrostatic charges of the four conformers examined for BAAM. Conformers **II**-**IV** have higher energy than **I**. Table 3 also includes the absolute (rms) and relative (rms_{rel}) root mean-square fits of the QM-calculated MEP to the classical model. The MEP was calculated at about 1800 points for each conformer. The rms and rms_{rel} values range between 0.9-1.1 kcal/mol and 5.2-7.9%, respectively, indicating a good fitting. Moreover, dipoles determined from electrostatic charges and from SCF wave functions exhibit a high degree of similarity.The presence of N-H electron withdrawal groups does not induce a positive charge in the α-carbon (C4) of the lowest energy conformation. Thus, the atomic charge on the α-carbon of **I** is approximately zero. However, when the typical structures of polypeptides are considered, a variation of the charge distribution with the conformation is observed. Thus, the change in the conformation leads to significant variations in the partial charge of those atoms buried within the central residue. The α-carbon becomes positive by the withdrawal of electrons through the N-H groups, varying from -0.05 to 0.46 . The neighboring N (N3 and N5) and H (H13 and H14) atoms display a range of variation of approximately 0.2 and 0.1, respectively. On the other hand, the remaining atoms present well-defined charges with a range of variation lower than 0.1.

Table 4 shows the results obtained for DMMA. In this case conformations **II**-**IV** are also strongly unstabilized. The good fitting between QM and classical MEPs is revealed in the small values of rms and rms_{rel}. The atomic point charge of the α-carbon (C4) has the highest negative value. This must be attributed to the electron donation by the neighboring carbonyl groups. A detailed study of the data indicates the same trend as in BAAM; only those atoms buried in the malonamide residue are sensitive to the environment, showing a range of variation greater than 0.1 eu. The α-carbon shows the largest variation, from 0.66 to -0.97. The carbon atoms of the carbonyl group (C3 and C5) and the hydrogens attached to the α-carbon (H13 and H14) show a variation of 0.2 and 0.1, respectively.

The results indicate a dependence of the atomic charges on the conformation, especially on the dipeptide backbone atoms. However, due to the restricted conformational space of BAAM[14] and DMMA,[17] this must not affect the ability of FF method to sample the conformational properties of these compounds. Thus, following the strategy developed by Richards and co-wokers[77] the charges evaluated from different conformations were weighted according to the Boltzmann populations. The weights are given by the standard Boltzmann formula using the 6-31G* energies of the geometries computed at

(61) Pearlman, D. P.; Kim, S. H. *Biopolymers* **1985**, *24*, 327.
(62) Momany, F. A. *J. Phys. Chem.* **1978**, *82*, 592.
(63) Connolly, M. *QCPE* **1981**, *1*, 75.
(64) Cox, S. R.; Williams, D. E. *J. Comput. Chem.* **1981**, *2*, 304.
(65) Singh, U. C.; Kollman, P. A. *J. Comput. Chem.* **1984**, *5*, 129.
(66) Luque, F. J.; Orozco, M.; Illas, F.; Rubio, J. *J. Am. Chem. Soc.* **1991**, *113*, 5203.
(67) Orozco, M.; Luqu, F. *J. Comput. Chem.* **1993**, *14*, 799.
(68) Alemán, C.; Luque, F. J.; Orozco, M. *J. Comput. Chem.* **1993**, *14*, 799.
(69) Alemán, C.; Luque, F. J.; Orozco, M. *J. Comput. Aided Mol. Design* **1993**, *7*, 721.
(70) Luque, F. J.; Orozco, M. *Chem. Phys. Lett.* **1990**, *168*, 269.
(71) Kikuchi, O.; Natsui, T.; Kozaki, T. *J. Mol. Struct. (THEOCHEM)* **1990**, *207*, 103.
(72) Williams, D. E. *Biopolymers* **1990**, *29*, 1367.
(73) Alemán, C.; Casanovas, J. *J. Chem. Soc., Perkin Trans. II* **1994**, 563.
(74) Stern, P. S.; Chorev, M.; Goodman, M.; Hagler, A. T. *Biopolymers* **1983**, *22*, 1901.
(75) IUPAC-IUB Commision on Biological Nomenclatures. *Biochemistry* **1970**, *9*, 3471.
(76) Hariharam, P. C.; Pople, J. A. *Thoret. Chim. Acta* **1973**, *28*, 213.
(77) Reynolds, C. A.; Essex, J. W.; Richards, W. G. *J. Am. Chem. Soc.* **1992**, *114*, 9075.

Table 3. Electrostatic Charges, Energies, and Fitting Results Computed from the 6-31G* Wave Functions for the Four Conformers of Bis(acetamido)methane

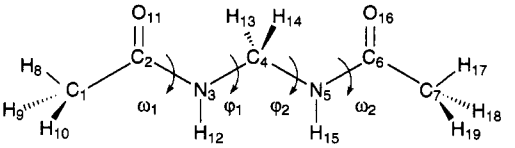

atom	I	II	III	IV	range[a]	I (MNDO)[b]
C1	−0.5268	−0.5111	−0.5082	−0.5337	0.0265	−0.6490
C2	0.8271	0.8022	0.8237	0.8754	0.0959	0.7055
N3	−0.5733	−0.7222	−0.7284	−0.7374	0.1840	−0.6484
C4	−0.0479	0.4942	0.4652	0.2158	0.5420	−0.0472
N5	−0.6042	−0.7594	−0.7588	−0.6236	0.1760	−0.6195
C6	0.8548	0.8257	0.8429	0.8766	0.0828	0.6771
C7	−0.5378	−0.5244	−0.5185	−0.5798	0.0669	−0.6194
H8	0.1434	0.1216	0.1252	0.1619	0.0403	0.1848
H9	0.1570	0.1584	0.1614	0.1552	0.0074	0.1844
H10	0.1225	0.1373	0.1301	0.1133	0.0239	0.1874
O11	−0.6393	−0.6143	−0.6391	−0.6479	0.0336	−0.4405
H12	0.3554	0.3531	0.3551	0.3976	0.0476	0.3387
H13	0.1516	0.0664	0.0969	0.0691	0.0852	0.1607
H14	0.1493	−0.0295	−0.0197	0.0849	0.1788	0.1573
H15	0.3705	0.3734	0.3733	0.3437	0.0301	0.3289
O16	−0.6306	−0.5969	−0.6256	−0.6293	0.0337	−0.4402
H17	0.1428	0.1418	0.1350	0.1667	0.0317	0.1795
H18	0.1544	0.1554	0.1577	0.1604	0.0087	0.1780
H19	0.1286	0.1282	0.1317	0.1311	0.0053	0.1819
ΔE^c	0.0	11.8	12.5	17.7		
$\mu_{SCF}{}^c$	1.44	7.90	7.94	3.94		0.84
$\omega_1{}^d$	175.7	180.0	180.0	180.0		175.7
$\varphi_1{}^d$	69.3	−119.0	−139.0	60.0		69.3
$\varphi_2{}^d$	67.4	113.0	135.0	30.0		67.4
$\omega_2{}^d$	176.2	180.0	180.0	180.0		176.2
N^e	1847	1882	1897	1780		1847
rms[f]	0.94	1.06	0.94	1.01		3.31
$rms_{rel}{}^g$	7.7	5.6	5.2	7.9		36.0
$\mu_{el}{}^h$	1.46	7.87	7.94	3.66		0.79

[a] Range of variation for each atom. [b] Electrostatic charges and fitting results computed for conformer I from a MNDO wave function following the procedure described in refs 63 and 64 (see text). [c] Relative energies (in kcal/mol) and dipole moments (in Debyes) computed from the SCF wave functions. [d] Torsional angles in degrees. [e] Number of points around each conformer used to compute the MEP. [f] Root-mean-square deviations (in kcal/mol) of the fitting of the Coulombic potential generated by the electrostatic charges to the QM electrostatic potential. [g] Relative root mean square deviations (in %) of the fitting of the Coulombic potential generated by the electrostatic charges to the QM electrostatic potential. [h] Dipole moments (in Debyes) computed from electrostatic charges.

room temperature (T = 298.15 K). As expected, the high energies of the typical structures of polypeptides made these multiple-conformation electrostatic charges the same as those for conformation **I**.

These results indicate that for BAAM and DMMA the charges derived on the minimum energy conformation at the SCF 6-31G* level must correctly describe the accessible conformational space of the molecules. However, the repetitive units of nylons 1,*n* cannot be considered at the ab initio 6-31G* level, owing to the large number of atoms. Consequently, the use of a less expensive strategy is required. In this respect Orozco and Luque[67-70] have developed strategies to compute the MEP from Dewar's[59,78] and Stewart's[79] semiempirical methods. The results demonstrated that Dewar's MNDO is an excellent source of electrostatic charges, and if suitable scaling procedures are used the agreement with the ab initio 6-31G* is excellent. The scaled (using a scaling factor of 1.32) MNDO electrostatic charges for conformation **I** of BAAM and DMMA are shown in Tables 3 and 4, respectively. They are in good agreement with the ab initio 6-31G* results. Electrostatic charges for all the compound studied in the present work were computed following the guidelines shown for model dipeptides. This was achieved using MNDO wave functions and weighting the electrostatic charges of the different conformations according to the Boltzmann populations. Results for the BAAE and BAAP dipeptides, and for the repetitive units of nylons 1,3 and 1,5, are shown in Figure 3.

van der Waals and 12-10 H-Bond Terms. Pairwise H-bond interactions are quite transferable. Furthermore, van der Waals atomic parameters are also quite transferable[43] and depend mainly on the atomic number and degree of hybridization. Thus, the nonbonded parameters related to the atoms of repetitive units of all the compounds under study have been considered equivalent to the other atoms already present in the AMBER FF for protein residues.

Test Cases: Bis(acetamido)methane and *N,N'*-Dimethylmalonamide. In order to elucidate the reliability of the parameters studied, we compared the heat capacity (constant volume) and molecular entropy (T = 298 K) for the BAAM and DMMA[90] model molecules computed from FF calculations with those obtained at the SCF AM1[59] level. Furthermore, in order to study the performance of the MNDO charges *vs* the 6-31G* ones, we used both sets of electrostatic parameters, which were denoted as FF/6-31G* (FF parameters with ab initio

(78) Dewar, M. J. S.; Thiel, W. *J. Am. Chem. Soc.* **1977**, *99*, 4899.
(79) Stewart, J. J. P. *J. Comput. Chem.* **1989**, *10*, 209.

Table 4. Electrostatic Charges, Energies and Fitting Results Computed from the 6-31G* Wave Functions for the Four Conformers of *N,N'*-Dimethylmalonamide

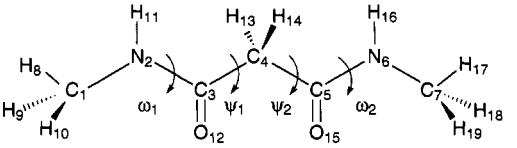

atom	I	II	III	IV	range[a]	I (MNDO)[b]
C1	−0.3232	−0.3442	−0.2944	−0.2790	0.0652	−0.2897
N2	−0.4147	−0.4172	−0.4710	−0.5258	0.1111	−0.4827
C3	0.7086	0.7589	0.8248	0.8499	0.1780	0.6450
C4	−0.6612	−0.6524	−0.8911	−0.8187	0.3130	−0.7252
C5	0.7620	0.7322	0.8412	0.8432	0.1135	0.6646
N6	−0.4427	−0.4398	−0.4671	−0.5152	0.0783	−0.5632
C7	−0.2634	−0.2911	−0.2946	−0.2659	0.0312	−0.1855
H8	0.1420	0.1437	0.1393	0.1326	0.0162	0.1321
H9	0.1464	0.1492	0.1371	0.1344	0.0142	0.1211
H10	0.1520	0.1571	0.1389	0.1370	0.0291	0.1486
H11	0.3167	0.3146	0.3316	0.3568	0.0422	0.3152
O12	−0.5942	−0.6338	−0.5960	−0.5928	0.0410	−0.4460
H13	0.2182	0.2256	0.1771	0.1435	0.1144	0.2324
H14	0.1665	0.1896	0.2968	0.2571	0.1303	0.1991
O15	−0.5937	−0.6153	−0.6070	−0.5949	0.0445	−0.4255
H16	0.3111	0.3213	0.3206	0.3477	0.0366	0.3298
H17	0.1219	0.1298	0.1420	0.1350	0.0257	0.1181
H18	0.1359	0.1354	0.1341	0.1269	0.0090	0.1160
H19	0.1213	0.1463	0.1377	0.1282	0.0250	0.0957
ΔE^c	0.0	25.9	30.2	34.5		
$\mu_{SCF}{}^c$	2.59	3.74	8.11	7.81		1.99
$\omega_1{}^d$	−179.7	180.0	180.0	180.0		177.3
$\psi_1{}^d$	111.5	60.0	−119.0	−139.0		108.7
$\psi_2{}^d$	52.7	30.0	113.0	135.0		47.4
$\omega_2{}^d$	−177.8	180.0	180.0	180.0		179.1
N^e	1826	1791	1837	1819		1826
rms[f]	1.04	1.01	0.90	0.86		3.22
$rms_{rel}{}^g$	8.7	7.4	4.4	4.3		34.9
$\mu_{el}{}^h$	2.59	3.77	8.11	7.28		1.82

[a] Range of variation for each atom. [b] Electrostatic charges and fitting results computed for conformer **I** from a MNDO wave function following the procedure described in refs 63 and 64 (see text). [c] Relative energies (in kcal/mol) and dipole moments (in Debyes) computed from the SCF wave functions. [d] Torsional angles in degrees. [e] Number of points around each conformer used to compute the MEP. [f] Root-mean-square deviations (in kcal/mol) of the fitting of the Coulombic potential generated by the electrostatic charges to the QM electrostatic potential. [g] Relative root-mean-square deviations (in %) of the fitting of the Coulombic potential generated by the electrostatic charges to the QM electrostatic potential. [h] Dipole moments (in Debyes) computed from electrostatic charges.

6-31G* electrostatic charges) and FF/MNDO (FF parameters with semiempirical MNDO electrostatic charges). Results are displayed in Table 5. Owing to the different treatment of frequencies in the calculation of S and C_v in THERMO(MOPAC) and NMODE(AMBER) modules, it is not possible to perform a direct comparison between SCF and FF data. Nevertheless, the qualitative agreement is remarkable between SCF and FF frequencies, which differ in general by around 2 cal/mol K. On the other hand, FF/6-31G* and FF/MNDO agree very well, as noted from the differences in entropies and heat capacities, which are seldom greater than 1 cal/mol.

The final test for any FF is obviously the comparison with experimental data. Accordingly, in order to validate the quality of the parameters derived in the previous section, we compared the MM-optimized geometries for the BAAM and DMMA with the available X-ray data.[10,15] This test is especially challenging since the crystalline environment was not considered in either the parametrization or the MM geometry optimizations. Results are given in Table 6. The comparison underlines the excellent ability of MM to reproduce experimental bond distances and angles.

Regarding dihedral angles, FF/6-31G* and FF/MNDO optimized structures of BAAM are in good agreement with the conformation obtained from both X-ray crystallography and ab initio calculations. This is located in the α_D catchment region of the $E(\varphi_1,\varphi_2)$ map[15] and corresponds to a helical conformation where close amide groups are oriented in opposite directions forming a single hydrogen bond direction. On the other hand, Table 6 shows a substantial difference between the X-ray crystallography and the theoretical ab initio conformations found for DMMA. Thus, when the symmetric *N,N'*-malonamide derivatives are packed in a crystal, both peptide groups are involved in the formation of inifinite hydrogen-bond systems, the optimal conformation appearing at $\psi_1 = \psi_2$. However, it is well known that in vacuum conditions the theoretical minimum appears in a region with $\psi_1 \neq \psi_2$, where a six-membered hydrogen-bond system is formed.[17] This asymmetric behavior is well represented from a qualitative point of view by both FF/6-31G* and FF/MNDO calculations, although the latter appears to underestimate this effect quantitatively.

Conformational Analysis of α-Alkylated and α,α-Alkylated Retro-Dipeptides: Bis(acetamido)ethane and Bis(acetamido)propane

The conformational preferences of *N,N'*-dimethyl-2-methylmalonamide and *N,N'*-dimethyl-2,2-dimethylmalonamide have recently been studied using semiem-

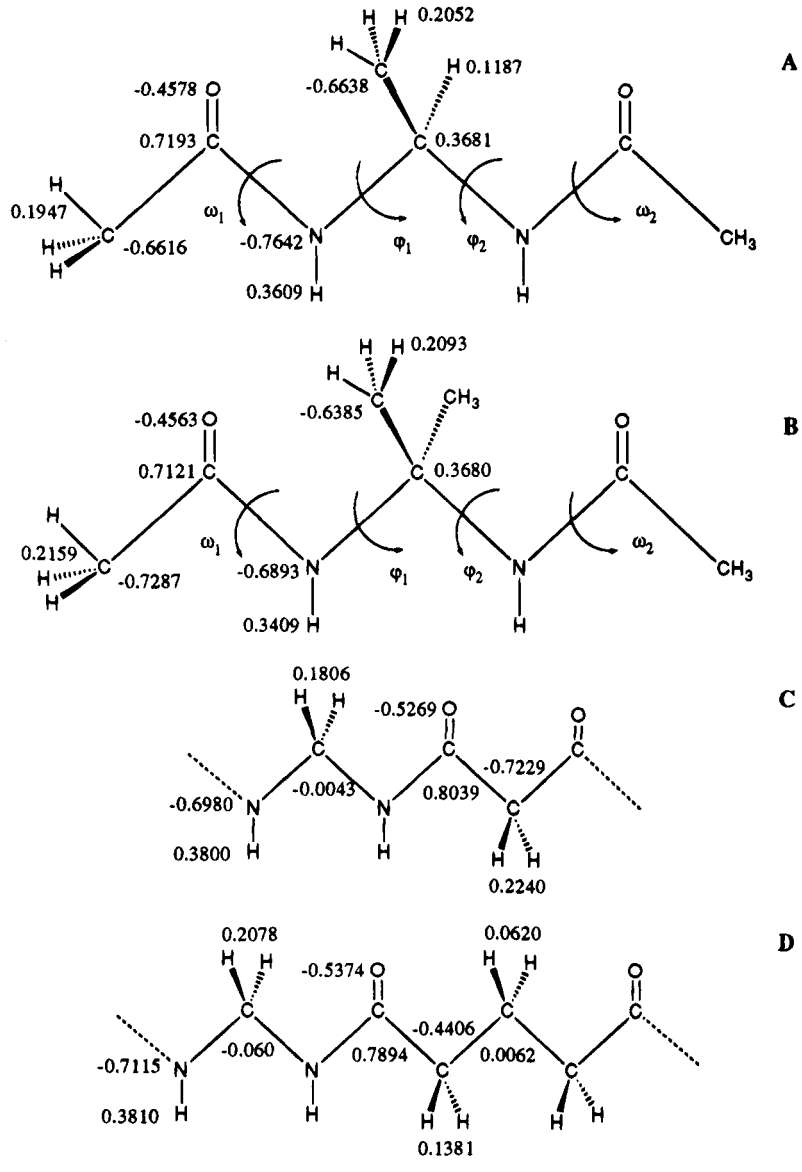

Figure 3. MNDO electrostatic atomic net charges computed for (A) bis(acetamido)ethane; (B) bis(acetamido)propane; (C) repetitive unit of nylon 1,3; (D) repetitive unit of nylon 1,5.

Table 5. Heat Capacities (in cal/mol·K) and Entropies (in cal/mol·K) for Bis(acetamido)methane and *N,N'*-Dimethylmalonamide Model Molecules at 298 K

molecule	parameter	SCF/ AM1	FF/ 6-31G*	FF/ MNDO
$CH_3CONHCH_2NHCOCH_3$	C_v	37.5	39.4	39.4
	S	108.2	108.7	108.4
$CH_3NHCOCH_2CONHCH_3$	C_v	37.6	39.3	39.2
	S	105.1	106.4	109.0

pirical QM methods.[18] However, little is known about the structural properties of bis(acetamido)etane (BAAE) and bis(acetamido)propane (BAAP), which can be considered as the ψ[CONH]-retro-peptides of alanine and α-aminoisobutyric acid (see Figure 3). A few years ago Stern et al.[19] computed the Ramachandran map of the BAAE using the Hagler–Huler–Lifson 9-6-1 potential.[80] The authors used a rigid-geometry approximation and found the minimum energy structures without full-geometry optimizations. Instead, the minima were located using a grid search procedure with a sweep of 20°.

(80) Hagler, A. T.; Huler, E.; Lifson, L. *J. Am. Chem. Soc.* **1974**, *96*, 5319.

Consequently, although the results provided an overall picture of the conformational map, the characterization of the low-energy structures was rather crude. In this section we continue our previous study about the conformational preferences of small *gem*-diamide derivatives.[14] We reinvestigate the potential energy surface as well as the conformational and energetic properties of BAAE and extend the study to BAAP, which to our knowledge has never been studied, using both QM and FF calculations.

Figure 4, part A, shows the potential energy surface $E(\varphi_1,\varphi_2)$ of the BAAE computed with the semiempirical AM1 method. A first inspection suggests that it is similar to that found for BAAM.[14] However, starting from different points of the conformational space, five minima were found for BAAE, whereas only two were found for BAAM. The eigenvalues of the hessian matrix were investigated for each of the minima, ensuring that all of them were positive. The relative energies and dihedral angles for all the minima characterized are listed in Table 7. The two lowest-energy structures, **Ia** and **Ib**, are equivalent with the same energy. These are located in the helical region of the Ramachandran map. Figure 5,

Table 6. X-ray (refs 10 and 15) and Theoretically Derived Bond Lengths (in Å) and Angles (in deg) for Bis(acetamido)methane and *N,N'*-Dimethylmalonamide[a,b]

distances	exp	FF/6-31G*	FF/MNDO	angles	exp	FF/6-31G*	FF/MNDO
				Bis(acetamido)methane[c]			
C1–C2	1.503	1.523	1.523	C1–C2–N3	116.6	116.6	116.6
C2–N3	1.336	1.338	1.338	C2–N3–C4	122.1	123.8	123.7
N3–C4	1.446	1.455	1.455	N3–C4–N5	112.7	108.1	108.7
C4–N5	1.446	1.454	1.455	C4–N5–C6	121.3	123.6	123.9
N5–C6	1.331	1.338	1.338	N5–C6–C7	115.8	116.6	116.5
C6–C7	1.502	1.522	1.523	O11–C2–C1	121.5	120.3	120.2
O11–C2	1.234	1.229	1.230	O16–C6–C7	122.3	120.3	120.2
O16–C6	1.226	1.229	1.230	ω_1	−178.2 (175.7)[d]	−179.5	−178.0
				φ_1	86.4 (69.3)[d]	81.0	75.9
				φ_2	83.8 (67.4)[d]	77.0	76.8
				ω_2	−178.2 (176.2)[d]	−179.4	−179.9
				N,N'-Dimethylmalonamide			
C1–N2	1.474	1.457	1.456	C1–N2–C3	121.5	121.5	123.2
N2–C3	1.314	1.335	1.334	N2–C3–C4	115.5	118.0	117.6
C3–C4	1.502	1.513	1.511	C3–C4–C5	109.8	118.7	118.0
C4–C5	1.502	1.514	1.511	C4–C5–N6	115.5	118.3	117.4
C5–N6	1.314	1.333	1.334	C5–N6–C7	121.5	122.8	122.2
N6–C7	1.474	1.456	1.453	O12–C3–N2	122.9	121.8	122.7
O12–C3	1.217	1.228	1.226	O15–C5–N6	122.9	122.2	122.6
O15–C5	1.217	1.227	1.226	ω_1	−175.7 (−179.7)[e]	176.7	179.1
				ψ_1	114.8 (111.5)[e]	146.9	80.4
				ψ_2	114.8 (52.7)[e]	31.5	67.1
				ω_2	−175.7 (−177.8)[e]	178.0	178.4

[a] FF/6-31G* means force field with ab initio 6-31G* electrostatic charges, and FF/MNDO means force field with semiempirical MNDO electrostatic charges. The dihedral angles obtained from ab initio geometry optimizations (refs 14 and 17) are also displayed. [b] The atom numbering is indicated in Tables 3 and 4. X-ray data of *N,N'*-dimethylmalonamide are not available, therefore the crystallographic data of the *N,N'*-dipropylmalonamide were used for comparison (ref 15). [c] The crystals of bis(acetamido)methane contain two molecules with slightly different geometrical parameters. The values shown in the table correspond to the average for the two molecules (ref 10). [d] Conformational angles obtained from ab initio geometry optimizations at the HF/6-31G* level (ref 14). [e] Conformational angles obtained from ab initio geometry optimizations at the HF/4–31G* level (ref 17).

Table 7. Semiempirical AM1, ab Initio 3-21G, and Molecular Mechanics Results Obtained for Bis(acetamido)ethane.[a] Relative Energies Computed at the 6-31G* Level Using the 3-21G Optimized Geometries Are Shown in Parentheses

label	level of geometry optimization	ω_1	φ_1	φ_2	ω_2	ΔE
Ia	AM1	−174.0	66.2	58.2	−174.7	0.0
	3-21G	−176.0	72.0	59.9	−175.3	0.0 (0.0)
	MM	179.7	53.1	82.7	178.3	0.0
Ib	AM1	174.6	−58.3	−66.0	174.7	0.0
	3-21G	174.9	−59.9	−72.1	176.1	0.0 (0.0)
	MM	178.4	−82.9	−53.6	179.9	0.0
II	AM1	−167.2	161.1	−57.4	179.5	4.3
	3-21G	167.9	166.2	−67.1	173.3	4.3 (3.1)
	MM	−178.9	151.5	−79.4	180.0	2.2
IIIa	AM1	169.6	126.1	−75.6	177.9	4.4
	3-21G	171.3	131.6	−78.6	−178.3	4.5 (3.7)
	MM	−179.9	143.6	−80.4	179.8	3.6
IIIb	AM1	−177.9	75.8	−125.6	169.4	4.4
	3-21G	−179.2	85.9	−126.9	173.9	4.5 (3.7)
	MM	177.6	−78.9	141.5	176.4	3.6

[a] Dihedral angles in degrees. Relative energies in kcal/mol.

part a, shows the stereodiagram of the **Ia** conformation. Structure **II** corresponds to a semiextended conformation with $\varphi_1,\varphi_2 = 161.1°,-57.4°$, which is 4.3 kcal/mol less stable than the helical conformations. This type of structure has also been found in some short peptides.[81] Finally, the highest minima, **IIIa** and **IIIb**, correspond to a conformation seldom found in protein residues. Indeed, φ_1,φ_2 angles are approximately halfway between those of **I** and **II**.

In order to validate the semiempirical minimum energy structures found, these conformations were reinvestigated using ab initio SCF-MO calculations with the 3-21G[49] basis set. Thus, the AM1-minimized structures were used as input and were fully relaxed at the ab initio level. Minimizations were continued until the maximum energy gradient dropped below 0.0008 kcal/mol·Å and the energy change over the last five iterations was less than 0.01 kcal/mol. The optimized 3-21G geometries were used for single point calculations with the 6-31G* [76] basis set. Results are showed in Table 7. The same relative order was provided by the different methods considered. Thus, the helical conformer was predicted to be the most stable. It can be seen that the AM1 method underestimates the relative stability of **II** and **III** with respect to the ab initio 6-31G* calculations. Thus, at the semiempirical level the separation between **I** and **II** is 4.3 kcal/mol, while 6-31G* single-point calculations on the 3-21G geometries reveal a relative energy of 3.1 kcal/mol.

Figure 4, part B, shows the potential energy surface $E(\varphi_1,\varphi_2)$ of BAAP computed with the AM1 method. The chemical symmetry of the molecule leads to an exact enantiomeric equivalence of the Ramchandran map with respect to the two diagonals. Starting from different points of the conformational space, eight minima were found. The relative energies and conformational angles of all the minima are listed in Table 8.

In this case the lowest-energy conformation **I** is also 2-fold degenerate. These structures can be located in the helical region of the Ramachandran map. A stereodiagram of the lowest-energy structure is given in Figure 5, part b. On the other hand, conformation **II** is 4-fold degenerate (IIa–IId). This is due to the chemical symmetry and achiral nature of the molecule, from which the pair φ_1,φ_2 is equivalent to the conformations: φ_2,φ_1; $-\varphi_1,-\varphi_2$; and $-\varphi_2,-\varphi_1$, *i.e.* when $\varphi_1 = \varphi_2$ as in **I** and **III** the unique equivalent conformation is $-\varphi_1,-\varphi_2$. These are 3.9 kcal/mol less stable than conformations **I** and cor-

(81) Toniolo, C.; Pantano, M.; Formaggio, F.; Crisma, C.; Bonora, G. M.; Aubry, A.; Bayeul, D.; Dautant, A.; Boesten, W. H.; Schoemaker, H. E.; Kamphuis, J. *Int. J. Biol. Macromol.* **1994**, *16*, 7.

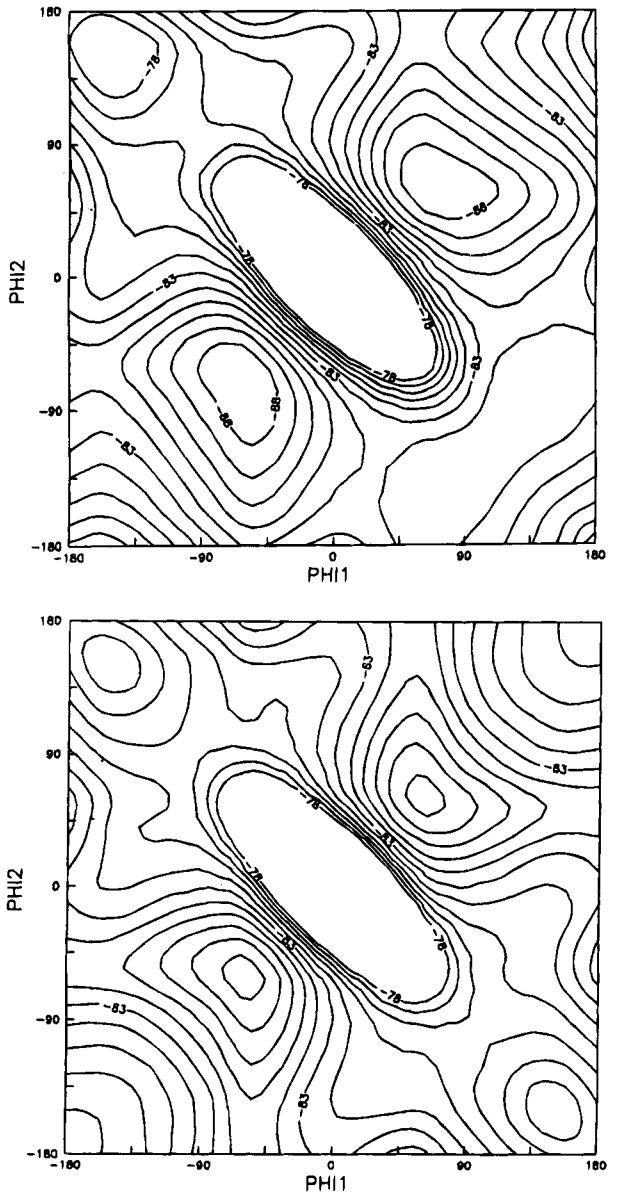

Figure 4. Potential energy surfaces for bis(acetamido)ethane (A) and bis(acetamido)propane (B) computed using the AM1 method. The isopotential lines are spaced by 1 kcal/mol.

respond to semiextended structures. Finally, the minima **III** adopt an extended conformation, which is 9.7 kcal/mol less stable than **I**.

Figure 3 reports the electrostatic charges from MNDO calculations for the two dipeptides. FF treatments of conformational flexible species are possible only if charges on equivalent nuclei are identical in terms of the simulation. For instance, all the hydrogens on a methyl group must bear the same charge, otherwise the three degenerate rotamers of the methyl would give rise to different energies. Thus, forcing symmetry in equivalent nuclei has been performed by averaging the corresponding charges. Tables 7 and 8 present the results obtained for the different conformers of BAAE and BAAP using MM calculations. The conformational angles and relative energies are in good agreement with QM calculations.

Finally, we should compare the results obtained for BAAE and BAAP with the conformations of dipeptides without retro-amide links *i.e.* alanine (Ala)[82-84] and

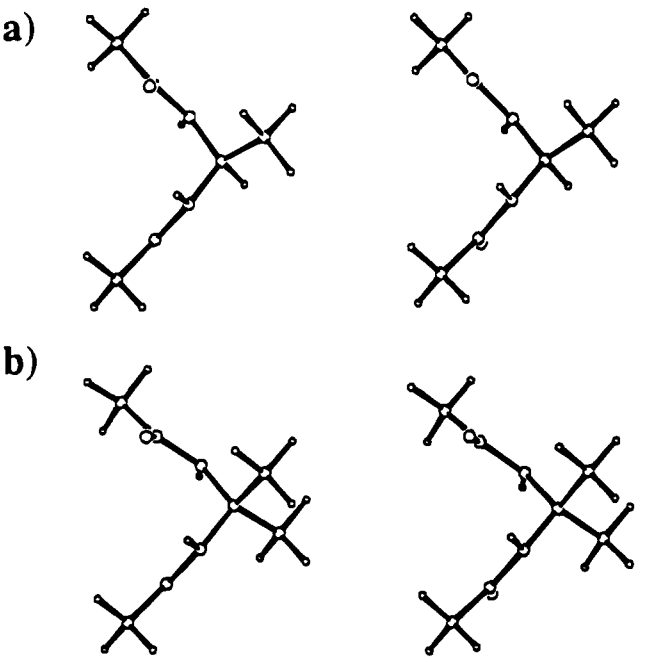

Figure 5. Representation of the lowest-energy structure of (a) bis(acetamido)ethane and (b) bis(acetamido)propane.

Table 8. Semiempirical AM1 and Molecular Mechanics Results for Bis(acetamido) propane[a]

label	level of geometry optimization	ω_1	φ_1	φ_2	ω_2	ΔE
Ia	AM1	−173.2	55.8	55.8	−173.4	0.0
	MM	−178.6	54.8	53.5	−178.3	0.0
Ib	AM1	173.3	−56.2	−55.9	173.4	0.0
	MM	178.6	−54.9	−58.7	−175.6	0.0
IIa	AM1	−178.2	53.9	177.1	169.0	3.9
	MM	178.7	56.2	178.5	178.5	1.4
IIb	AM1	−168.9	177.2	54.0	−174.4	3.9
	MM	−171.5	169.4	59.7	179.9	1.4
IIc	AM1	−168.7	−178.0	−54.0	178.2	3.9
	MM	−175.7	−174.5	−57.9	−178.4	1.4
IId	AM1	178.3	−54.1	−176.9	−170.0	3.9
	MM	176.5	−59.8	−169.8	178.9	1.4
IIIa	AM1	170.7	176.8	175.8	170.9	9.7
	MM	179.9	179.1	177.9	−179.6	4.9
IIIb	AM1	173.1	−174.6	−176.1	−174.2	9.7
	MM	180.0	−179.9	−171.6	−179.9	4.9

[a] Dihedral angles in degrees. Relative energies in kcal/mol.

α-aminoisobutyric acid (Aib).[85-88] A notable feature is the stabilization in retro-peptides of the helix conformation, which is the less favored minimum in Ala and Aib. Thus, owing to the retro-amide link, some of the well-established minimum-energy conformations for nonmodified amino acids were not found in BAAE and BAAP, *e.g.* C_5 (intramolecular five-membered hydrogen-bonded system) in BAAE and C_7 (seven-membered hydrogen-bonded system). This illustrates the important effects induced by retromodification of an amide link in the potential-energy surface of a residue.

(82) Böhm, H. J.; Brode, S. *J. Am. Chem. Soc.* **1991**, *113*, 7129.
(83) Head-Gordon, T.; Head-Gordon, M.; Frisch, M. J.; Brooks, C. L., III; Pople, J. A. *J. Am. Chem. Soc.* **1991**, *113*, 5989.
(84) Gould, I. R.; Kollman, P. A. *J. Phys. Chem.* **1992**, *96*, 9255.
(85) Paterson, Y.; Rumsy, S. M.; Benedetti, E.; Nemethy, G.; Scheraga, H. A. *J. Am. Chem. Soc.* **1981**, *103*, 2947.
(86) Barone, V.; Fraternali, F.; Cristinziano, P. L. *Macrolecules* **1990**, *23*, 2038.
(87) Alemán, C.; Pérez, J. J. *Int. J. Quantum Chem.* **1993**, *47*, 231.
(88) Alemán, C.; Casanovas, J. *J. Chem. Soc., Perkin Trans. 2* **1994**, 563.

Table 9. Conformational Parameters, Hydrogen-Bond Geometry, and *R* Factors for the Three Models of Nylons 1,3 and 1,5

	nylon 1,3			nylon 1,5		
	I	**II**	**III**	**I**[a]	**II**[a]	**III**
space group	$P6_522$	$P3_212$	Pm	$P6_522$	$P3_212$	Pm
cell parameters						
a (Å)	4.79	4.79	4.79	4.79	4.79	4.79
b (Å)	4.79	4.79	6.0[b]	4.79	4.79	8.7[b]
c (Å)	36.0[b]	18.0[b]	4.79	26.1[b]	52.2[b]	4.79
α (deg)	90	90	90	90	90	90
β (deg)	90	90	120	90	90	120
γ (deg)	120	120	90	120	120	90
torsional angles (deg)[c]						
φ_1	85.8	75.0	−100.4	87.1	88.0	−107.0
φ_2	85.8	75.0	100.4	87.1	88.0	107.0
ψ_1	−118.7	−145.6	−91.4	−119.9	−157.4	−98.5
ψ_2	−118.7	−145.6	91.4	−119.9	−157.4	98.5
H-bond geometry						
d(H···N) (Å)	1.64	1.80	1.73	1.64	1.86	1.75
d(N···O) (Å)	2.60	2.79	2.67	2.62	2.82	2.72
∠NHO (deg)	156	166	154	164	159	161
R factor (%)[d]	49.1	20.3	33.9	33.9	18.8	27.8

[a] Data from ref 28. [b] Fiber identity period. *b* axis for monoclinic lattices and *c* axis for hexagonal lattices. [c] Only the values of torsional angles different from 180° are given. [d] From electron diffraction data.

Crystalline Structure of Nylons 1,3 and 1,5

The structure of a series of nylons 1,*n* where *n* is even, has recently been determined by several methods, including X-ray diffraction and electron microscopy.[28] A new conformation that is different from conventional polyamides has been found. In the proposed model the values of the torsional angles φ_i ($\varphi_1 = \varphi_2 = +87.5°$ or $-87.5°$) were close to those observed[18] and calculated[14] for some methylene diamides, whereas the dicarboxylic moiety assumes a conformational arrangement $s^-t_{n-2}s^+$ similar to that found in the γ form of nylons.[22] Their crystalline structure is characterized by a monoclinic unit cell and a *B2/b11* space group, which explain the *2/mmm* symmetry of the electron diffraction patterns. A single hydrogen-bond direction is also deduced from molecular conformation, justifying the growth direction of the lamellar crystals. In contrast, nylons 1,5[28] and 1,3[25] (see Figure 3) crystallize as hexagonal multilamellar aggregates and as doughtnut-like morphologies, respectively. Additionally, these aggregates always diffract like single crystals, exhibiting a hexagonal diffraction pattern with *6/mmm* symmetry. Two models can be proposed for each nylon, which correspond to a hexagonal packing of 6-fold and 3-fold helices (Figure 6 parts a−d). These conformations can be generated when the torsional angles of the methylene diamide unit are close to their low-energy values ($\varphi_1 = \varphi_2 = 80 \pm 15°$) and the carboxylic moiety takes a particular conformation. So $\psi_1 = \psi_2 \approx -120°$ (model **I**) and $\psi_1 = \psi_2 \approx -150°$ (model **II**) produce a rotation of 120° and 60°, respectively, between the C=O directions.

The structural investigation of models **I** and **II** for nylons 1,5 and 1,3 was carried out with the LALS method.[31] The results are summarized in Table 9. Both models were found without significant contacts and, therefore, appear stereochemically acceptable. All hydrogen bonds are allowed to form with length and angle values within the standard ranges and oriented according to three planar directions. Both models give a *6/mmm* symmetry for the *hk*0 electron diffraction pattern, although the calculated *R* factor is clearly favorable for model **II**.

Due to the limited number of spots used in the calculations, the conformational analysis carried out with the LALS method may not be determinant. So, in this work we report results of a packing analysis performed by energy calculations on the different models of nylons 1,5 and 1,3 with the aim of ascertaining both their relative stability and the reasons for such stability. In addition, these calculations permit us to validate the QM-derived FF. Thus, we have also generated a third model (Figure 6, parts e and f) to test the energy calculations. This model is based on the characteristic γ structure observed in polyamides from diamines with odd numbers of methylene groups and dibasic acids with odd numbers of methylene groups.[22] Thus, torsional angles are close to the expected values for a characteristic γ structure: $\varphi_1 = -\varphi_2 \approx 120°$ and $\psi_1 = -\psi_2 \approx 120°$. Indeed, the space group *Pm* cannot explain, in this case, the *6/mmm* symmetry of the diffraction pattern, and the calculated *R* factor shows a clear disagreement between the model and experimental data (see Table 9).

MM calculations were performed by taking into account the interactions with neighboring chains in the crystal. Initially, we generate of polymer chain of six monomeric residues, which were blocked at the amino end with an acetyl group and with an *N*-methylamide at the carbonyl end. Then, the hexagonal crystal environment was mimicked by considering a set of 30 polymer chains arranged according to the space groups of the three models investigated, *i.e.* $P6_522$ for model **I**; $P3_212$ for model **II**; and *Pm* for model **III**. Figure 7 shows the 14 hexagonal unit cells, *i.e.* a central chain surrounded by six chains, included in these systems. Minimizations were carried out without any symmetry constraint and by considering both conformational and packing terms:

$$E_{TOT} = E_{conf} + E_{pack} \quad (3)$$

The conformational term refers to the optimization of each chain. On the other hand, the packing energy has been calculated by taking into account the nonbonded interactions between the atoms of one chain and all the atoms of the surrounding chains. In order to avoid the end effects on the conformation, only the two middle residues of the four central hexagonal unit cells were considered when analyzing the information and, in addition, their dihedral angles were averaged. On the

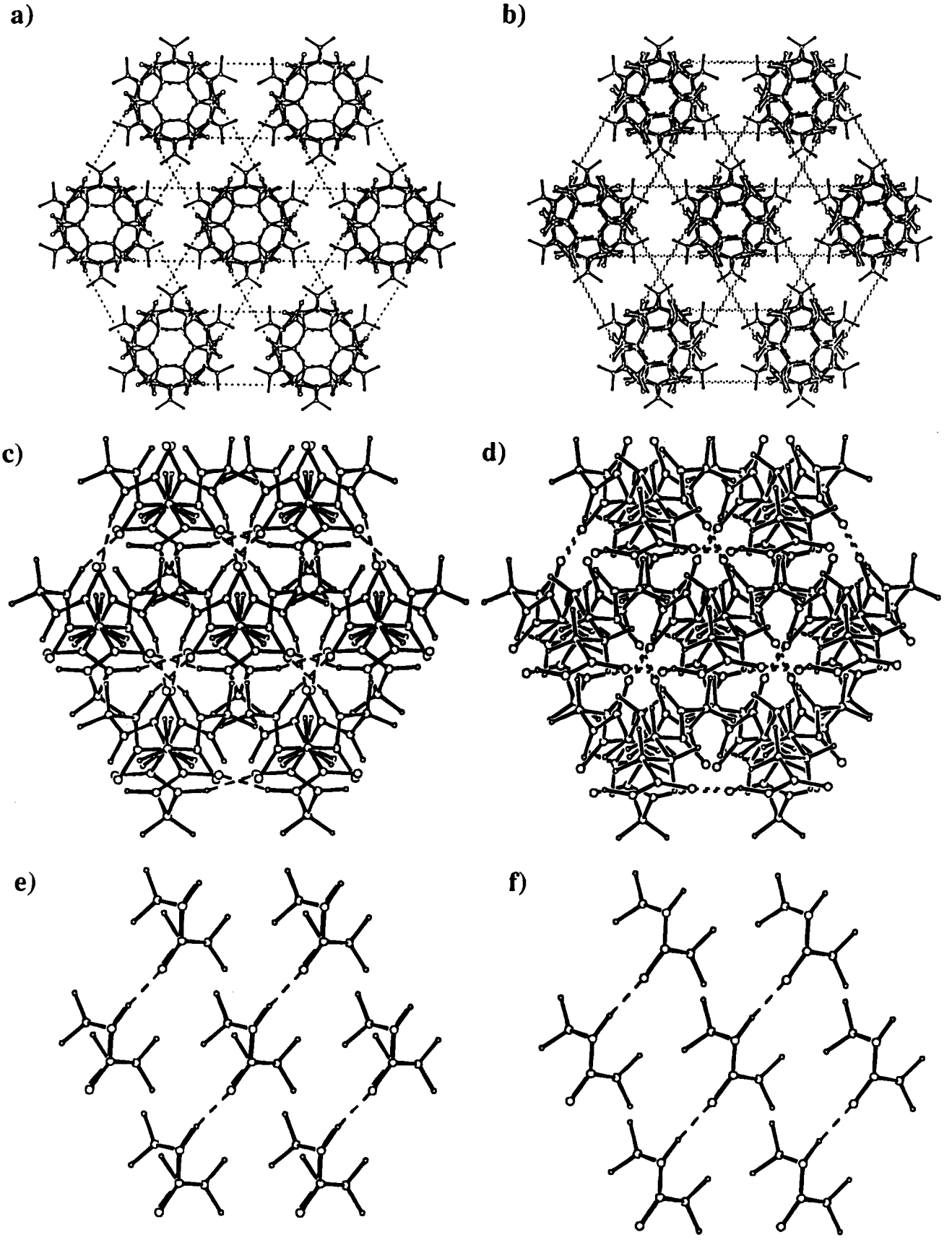

Figure 6. Equatorial projections of a centered molecule and six surrounding neighbors. Model **I**: (a) nylon 1,3 and (b) nylon 1,5. Model **II**: (c) nylon 1,3 and (d) nylon 1,5. Model **III**: (e) nylon 1,3 and (f) nylon 1,5. Molecular chains have been drawn in model **I** with an increased separation between them in order to show hydrogen bonds more clearly.

other hand, energy contributions[91] by residue were computed and averaged for the same residues.

MNDO electrostatic charges obtained for the monomeric units of nylons 1,3 and 1,5 are shown in Figure 3. Geometry optimizations were carried out in several steps. First, the starting conformations were subject to 350

Table 10. Conformational Angles[a] (in deg) and Crystallographic Parameters[b] (in Å and deg) Obtained from the Energy Minimization of Models I and II for Nylons 1,3 and 1,5

		conformational parameters								crystallographic parameters					
model		ω_1	φ_1	φ_2	ω_2	ψ_1	v_1	v_2	ψ_2	a	b	c	α	β	γ
nylon 1,3	I	170.9	80.8	97.9	178.7	−126.6			−107.3	4.67	4.81	38.1	87.1	93.0	116.5
	II	175.6	92.1	97.3	178.6	−152.2			−148.2	4.77	4.79	18.2	89.9	89.0	118.2
nylon 1,5	I	176.8	104.1	123.2	177.1	−146.9	174.1	−174.4	−128.5	4.69	4.78	27.8	86.7	105.0	115.4
	II	174.2	97.8	91.7	176.7	−164.1	−174.4	174.1	−161.3	4.74	4.73	51.3	89.3	90.7	117.6

[a] See Figure 3. [b] See Figure 7.

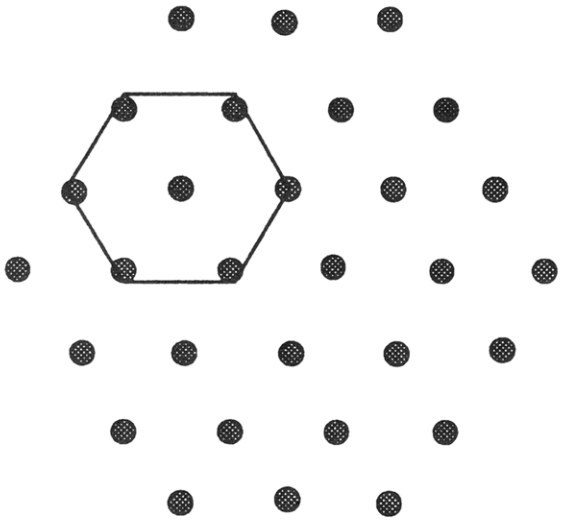

Figure 7. Equatorial projection of the system investigated by molecular mechanics. Each dot represents a polymer chain; 30 molecules were considered in order to mimic the packing interactions.

cycles of steepest descent optimization to eliminate the worst steric conflicts. Second, subsequent optimization using a conjugate gradient algorithm was performed until convergence. We imposed a 7.5 Å cutoff for the nonbonded interactions and updated the list of these interactions every 25 steps. A dielectric constant of $\epsilon = 1$ was used in energy optimization calculations.

The optimized values of the conformational angles and the crystallographic parameters obtained for models **I** and **II** of nylons 1,5 and 1,3 are reported in Table 10. The results are in accordance with the experimental observations (Table 9), especially for model **II**, where all the crystallographic parameters maintained the hexagonal symmetry. The values of the parameters obtained by geometry optimization for model **I** present some distortions. Thus, the final values of β and γ depart slightly from 90° and 120°, respectively. Furthermore, the optimized values of the c axis, which correspond to the chain length repeat, were increased approximately 2 Å with respect to the experimental data. On the other hand, dihedral angles obtained for model **II** preserved the molecular symmetry usually found in adirectional molecules *i.e.* $\varphi_1 = \varphi_2$ and $\psi_1 = \psi_2$. In contrast, optimized conformational parameters for model **I** reveal a distortion of the molecular symmetry. Thus, φ_1 and ψ_1 differ by about 20° from φ_2 and ψ_2, respectively, for both nylons 1,3 and 1,5. Consequently, model **II** better preserves the conformation for both polymers. Finally, model **III** is energetically unstable, and the geometry optimization led to a new structure in which no regular hydrogen-bonding geometry was found.

Table 11 shows the energy contributions computed for the different models. The results indicate that the energy of model **II** is lower than that of model **I** for each polymer

Table 11. Energy Contributions[a] (in kcal/mol·residue) Obtained from the Energy Minimization of Models I and II for Nylons 1,3 and 1,5

	model	E_{bonded}	E_{vdW}	E_{elec}	E_{12-10}	E_{TOT}	ΔE
nylon 1,3	I	2.7	−9.8	−44.0	−0.8	−51.9	1.5
	II	2.5	−8.6	−46.7	−0.6	−53.4	0.0
nylon 1,5	I	2.4	−9.2	−22.9	−0.7	−30.4	0.7
	II	2.2	−9.3	−23.3	−0.7	−31.1	0.0

[a] The different energy terms refer to one residue, where E_{bonded} = bonding energy, E_{vdW} = van der Waals energy, E_{elec} = electrostatic energy, E_{12-10} = energy corresponding to the $r^{-12} - r^{-10}$ term, E_{TOT} = total energy, and ΔE = relative energy.

considered. The analysis of the different contributions reveals similar trends for nylons 1,3 and 1,5. Thus, model **II** is favored by electrostatic interactions in all cases, whereas van der Waals contribution only favored model **II** in nylon 1,5. On the other hand, bonded and 12−10 contributions are similar in all cases. These results are in excellent agreement with our previous findings, which indicate that in polymers with a high ratio of amide to methylene groups the accounting of hydrogen-bonding interactions with neighboring molecules is essential.[30,89]

These results are in excellent agreement with those obtained from the X-ray data refinement using the LALS methodology, which indicate that for nylons 1,3 and 1,5 the helical structure with a 3-fold axis is favored (Table 9). What is clearly apparent is that the dihedral angles φ_1 and φ_2 obtained for the polymeric systems are very similar to those found in the above sections for the small model compounds, *i.e.* BAAM, BAAE, and BAAP. Thus, calculations *in vacuo* provided a minimum with conformational angles $\varphi_1 = \varphi_2 \approx \pm 70°$. On the other hand, when the crystal environmental effects were included in the calculations, the torsional angles changed by approximately 20°. Thus, this particular conformation of the bis(acetamide) residues seems to be preserved in both the small model compounds and the polyamides such as nylons 1,3 and 1,5. Finally, it should be noted that the γ form was not favored from an energetic point of view. Indeed, the intermolecular hydrogen-bonding scheme was disrupted by the geometry optimizations, making a new conformation without any kind of internal symmetry.

Conclusions

We studied the chemical and structural aspects of some types of retro-amide compounds, *i.e.* dipeptide and aliphatic polyamides. First, we investigated the pure interactions usually found in empirical FFs in order to

(89) Alemán, C.; Pérez, J. J. *J. Comput.-Aided Mol. Design* **1993**, *7*, 241.

(90) X-ray data of *N,N'*-dimethylmalonamide are not available, and consequently the crystallographic data of the *N,N'*-dipropylmalonamide were used for comparison.

(91) The different energy terms refer to those shown in eq 1, where both intra- and inter-residue interactions were taken into account.

provide an adequate set of parameters that permit the use of FF-based methods. The parametrization was performed using QM methods due to the lack of experimental information. Second, we extended our previous study about the conformational properties of retro-amide dipeptides to BAAE and BAAP. This was performed using both QM and MM methods. Finally, the crystalline structure of several aliphatic polyamides, which could be considered as models of nylons 1,*n* and *n*,3 were investigated. Thus, all the models compatible with the X-ray data were refined using both FF and LALS calculations. The results of this work give a series of conclusions on the effect of the inversion of the amide group on the conformation:

(1) Stretching and bending parameters found from QM calculations for residues with a retro-amide bond are similar to those provided for glycine in AMBER FF. That is, they do not depend on details of the structural moieties in which they are found. Thus, stretching and bending force constants are totally transferable between residues with a retro-amide link and those usually found in proteins. On the other hand, we found a notable agreement between force constants derived at the HF/3-21G level and those provided in empirical FFs, even though the former are usually larger because calculations at the HF level suffer from deficiencies. Moreover, comparison between empirical FFs indicates that a finer parametrization of the bending term was considered unnecessary.

(2) The profiles obtained for the rotation around the N−CT and C−CT from AM1 calculations in retro-peptides lead to high-energy barriers. However, the application of the correction method implemented in the PAPQMD strategy leads to results lying within the range of variation of the experimental data used in the different empirical FFs. These results suggest that conformational preferences in retro-peptides are principally governed by van der Waals and electrostatic interactions.

(3) The results of the electrostatic parametrization indicate that the changes in the charge distributions induced by the retromodification are dependent on which peptide group has been inverted. Thus, electron donation by the C=O groups in DMMA makes the α carbon more negative for all the conformations considered, whereas electron withdrawal by the N−H groups in BAAM makes the α carbon positive, but only in the less favored conformations. This result suggests that for BAAM the effects of the N−H groups tend to cancel when the conformation is the energy minimum or is located in its vicinity.

(4) The electrostatic charges computed from semiempirical MNDO MEPs and scaled to reproduce ab initio 6-31G* QM MEPs are able to represent the electrostatic distribution of molecules properly. Thus, comparison between FF/MNDO and FF/6-31G* demonstrated that the results obtained are similar. Furthermore, the scaled MNDO charges are powerful in MM studies of aliphatic polyamides where the size of the monomeric units makes ab initio parametrization difficult.

(5) The potential energy surfaces of BAAE and BAAP have been investigated using both the QM and FF methods. They contain five and eight minima, respectively. The lowest-energy conformations are in good agreement with those observed for BAAM. These conformations are of helical nature, and peptide and retro-peptide units point in opposite directions. A comparison of the results obtained here with the potential energy surfaces of Ala and Aib residues has been performed. The results indicate that modification of a usual residue in a polypeptide chain by its retro analog with formation of *gem*-diamide units results in a substantial conformational change.

(6) The crystalline structures of nylons 1,3 and 1,5, which can be considered to be models of nylons 1,*n* and *n*,3, have been investigated using the MM and LALS methods. The results reveal that the characteristic γ structure is not appropiate for this kind of compound. Thus LALS calculations show the poor agreement of the γ form with experimental data, whereas energy calculations reveal its low estability. On the other hand, both LALS and MM calculations indicate that a 3-fold helical conformation responsible for three hydrogen-bond directions seems to be the most stable for nylons 1,3 and 1,5.

(7) Finally, in all cases the compounds investigated, *i.e.* small dipeptides and aliphatic polyamides, present the lowest-energy minima near the helical regions of the Ramachandran map. Thus, the insertion of *gem*-diamide units could be useful for the stabilization of helical conformations in the design of polypeptides with a defined conformation.

Acknowledgment. El Centre de Supercomputació de Catalunya (CESCA) is gratefully acknowledged for computer time. We also thank Drs. M. Orozco and F. J. Luque for the use of computational facilities. This work has been supported by QFN 91-4204 (CIRIT,-CICYT) and PB91-0588 (DGICYT).

JO941261S